ELSEVIER

Journal of Alloys and Compounds 450 (2008) 395–399

Journal of ALLOYS AND COMPOUNDS

www.elsevier.com/locate/jallcom

SEM and TEM characterization of magnesium hydride catalyzed with Ni nano-particle or Nb_2O_5

Nobuko Hanada [a,1], Enoki Hirotoshi [b], Takayuki Ichikawa [a,*], Etsuo Akiba [a,b], Hironobu Fujii [a]

[a] *Institute for Advanced Materials Research, Hiroshima University, 1-3-1 Kagamiyama, Higashi-Hiroshima 739-8530, Japan*

[b] *National Institute of Advanced Industrial Science and Technology (AIST), AIST Central-5, 1-1-1 Higashi, Tsukuba, Ibaraki 305-8565, Japan*

Received 6 September 2006; received in revised form 26 October 2006; accepted 28 October 2006
Available online 4 December 2006

Abstract

The microstructures of MgH_2 catalyzed with Ni nano-particle or Nb_2O_5 mesoporous powders are examined by scanning electron microscopy (SEM) and transmission electron microscopy (TEM) observations. For MgH_2 catalyzed with Ni, the Ni particles with the diameter smaller than 1 μm were detected on the MgH_2 particles with the diameter smaller than 5 μm by the back scattering electron (BSE) microscopy. In details, the TEM micrograph indicates that the Ni particles distribute ∼20 nm in diameter on MgH_2 uniformly, which was the same size as the additive doped in MgH_2 before milling. On the other hand, for MgH_2 catalyzed with Nb_2O_5, the additive particles could not be found anywhere in the BSE image. Even in the TEM micrograph by much larger magnification than the SEM micrograph, the particles corresponding to the additive cannot be observed at all. Furthermore, an energy dispersive X-ray (EDX) analysis in spots with a diameter of 20 nm indicated that the existing ratio of Mg to Nb was evaluated to 98:2, being the same as the starting ratio before milling. Therefore, the metal oxide Nb_2O_5 becomes extremely small particle that could not be observed by the present work after milling compared to metal Ni^{nano}.

Keywords: Hydrogen absorbing materials; Ball-milling; Microstructure; Scanning electron microscopy (SEM); Transmission electron microscopy (TEM)

1. Introduction

Magnesium hydride MgH_2 has been considered as one of attractive hydrogen storage materials because it possesses a high hydrogen capacity of 7.6 mass% and abundant resources. However, the reaction speed of hydrogen absorption and desorption is too low since Mg has no strong catalytic effect for dissociation of hydrogen molecule into the atoms on the surface vice versa. Therefore, it needs a higher temperature than 300 °C for the hydrogen desorption under 0.1 MPa hydrogen pressure. Recently, in order to improve the kinetics of hydrogen absorption/desorption reactions without a significant reducing the high hydrogen capacity, Mg or MgH_2 doped with a small amount of some transition metals or transition metal oxides prepared by ball-milling have been studied [1–11].

Similarly, in our research group, MgH_2 composites with a small amount of some transition metals or transition metal oxides have been prepared by the ball-milling method and have been studied with respect to the hydrogen storage properties [12–15]. The MgH_2 composite with 2 mol% Ni nano-particle (MgH_2–Ni^{nano}) prepared by ball-milling at 200 rpm for 15 min hereafter defined as a short time milling desorbed ∼6.5 mass% hydrogen in the temperature range from 150 to 250 °C at heating rate of 5 °C/min [12–14]. Furthermore, the MgH_2 composite with 1 mol% Nb_2O_5 (MgH_2–Nb_2O_5) prepared by ball-milling at 400 rpm for 20 h hereafter defined as a long time milling desorbed ∼6.0 mass% hydrogen in the temperature range from 150 to 250 °C at heating rate of 5 °C/min after second cycle [13,14]. Thus, both of the products showed similar hydrogen desorption properties even though the milling conditions between

* Corresponding author. Tel.: +81 82 424 5744; fax: +81 82 424 5744.
E-mail address: tichi@hiroshima-u.ac.jp (T. Ichikawa).
[1] Current address: Karlsruhe Research Center, Institute of Nanotechnology, D-76021 Karlsruhe, Germany.

0925-8388/$ – see front matter © 2006 Elsevier B.V. All rights reserved.
doi:10.1016/j.jallcom.2006.10.128

two composites were quite different. Particularly, it is of interest that the MgH_2–Nb_2O_5 composite after dehydrogenation at 200 °C absorbed gaseous hydrogen of ~4.5 mass% even at room temperature under hydrogen gas pressures lower than 1 MPa within 15 s and finally its capacity reached up to more than 5 mass% after exposing hydrogen gas atmosphere for 8 h [15].

To characterize the catalyst in these composites, the X-ray diffraction (XRD) and X-ray absorption spectroscopy (XAS) measurements have been performed as well. For the MgH_2–Ni^{nano} composite, the additive was detected as Ni metal phase by XRD measurement [12]. On the other hand, for both the MgH_2–Nb_2O_5 composites after milling and dehydrogenation, any traces corresponding to the Nb related phases could not be confirmed in the XRD profiles. This indicates that the additive is dispersed in MgH_2 in a nanometer scale by the ball-milling treatment and acts as a catalyst [13,14]. In addition, the characterization of the catalyst in the MgH_2–Nb_2O_5 composite has been investigated by the XAS measurement [16]. The result indicated that the X-ray absorption near edge structure (XANES) spectrum in the Nb K-edge for the sample coincides with that of NbO, where the valence number of the transition metal is approximately two. Therefore, the additive is reduced to other state of metal oxide by MgH_2, which is in a lower valence state than that of the starting material (Nb_2O_5).

In this work, the microstructures of the additives for the composites MgH_2 catalyzed with Ni^{nano} and Nb_2O_5 are investigated by using scanning electron microscopy (SEM) and transmission electron microscopy (TEM) observations to clarify the relation between the geometry of the catalyst such as the size and distribution and hydrogen storage properties.

2. Experimental procedures

Magnesium hydride MgH_2 powder (the purity is 90 mass%, 9 mass% is unreacted Mg and the rest is impurities; the size is several 10 μm) was purchased from Sigma–Aldrich. The nanometer-particle metal Ni^{nano} with a diameter of several 10 nm was from Shinku-Yakin, and niobium oxide Nb_2O_5 of mesoporous with 3.2 nm pore size (99.5% purity) was from Sigma–Aldrich.

The mixture of 300 mg MgH_2 and 2 mol% Ni^{nano} or 1 mol% Nb_2O_5 were put into a Cr steel pot (3×10^{-5} m^3 in volume) together with 20 steel balls (7 mm in diameter). Then, the inside of the pot was degassed below 1×10^{-4} Pa for 12 h and high-purity hydrogen gas (7 N) of 1.0 MPa was introduced into it. By using a planetary ball-milling apparatus (Fritsch P7), the MgH_2–Ni^{nano} composite was mechanically milled for 15 min at the rotating speed of 200 rpm and the MgH_2–Nb_2O_5 composite was milled for 20 h at 400 rpm. The samples before and after ball-milling were always handled in a glovebox filled with a purified Ar gas so as to minimize the oxidation on the samples. To synthesize dehydrogenated states of the MgH_2–Nb_2O_5 composite, the ball milled product was dehydrogenated under a high vacuum condition for 8 h at 200 °C.

Microstructure was observed by SEM equipped with an energy dispersive X-ray (EDX) apparatus (JEOL JSM-6380A) and TEM with EDX apparatus (JEOL JEM-2000FXII). The specimen was prepared by spreading the powders on the carbon seals for SEM and the collodion film supported on copper grid for TEM. Both the specimens were exposed in air for about 1 min to the mounting on the sample holder and subsequent connection to the microscope (SEM and TEM). To avoid the electrification, the SEM measurement was performed at a voltage of 5 kV.

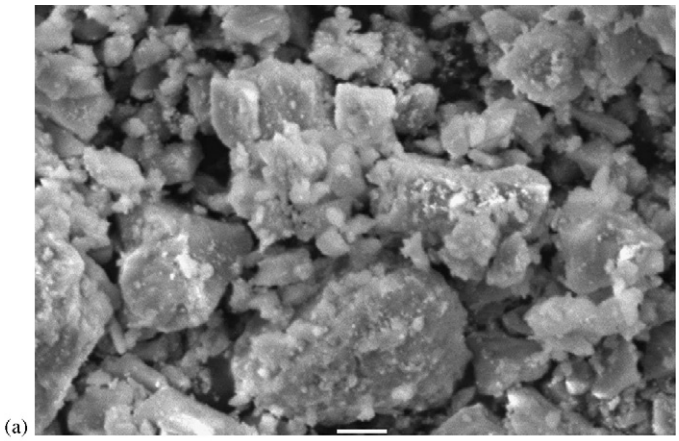

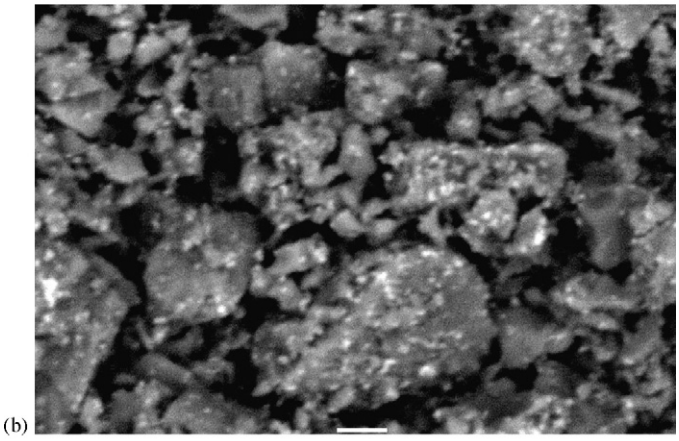

Fig. 1. (a) Secondary electron (SE) and (b) back scattering electron (BSE) images of the MgH_2–Ni^{nano} composite, in which both the (a) and (b) micrographs are taken in the same field.

3. Results and discussion

3.1. Microstructure of MgH_2 catalyzed with Ni^{nano} (MgH_2–Ni^{nano} composite)

Fig. 1(a) and (b) show, respectively, secondary electron (SE) and back scattering electron (BSE) images for the MgH_2–Ni^{nano} composite prepared by ball-milling for 15 min at 200 rpm. In the SE micrograph (Fig. 1(a)), various sized particles exist in the range of less than 1 μm to more than 5 μm. Because the milling time and milling speed are not long and high enough under our trial conditions, the powder size is not homogeneous and large sized particles are still present in the powder. In BSE image (Fig. 1(b)), which is the same area as the SE image, small sized particles with <1 μm in diameter are bright and uniformly distributed on the large sized particles. The BSE signals for the heavier element or the composite contained heavier element can be detected as much brighter spots. Therefore, the bright part shows the distribution of Ni particles because Mg has much smaller atomic number. This indicates that the Ni particles homogeneously distribute in such a micrometer scale range on the surface of MgH_2.

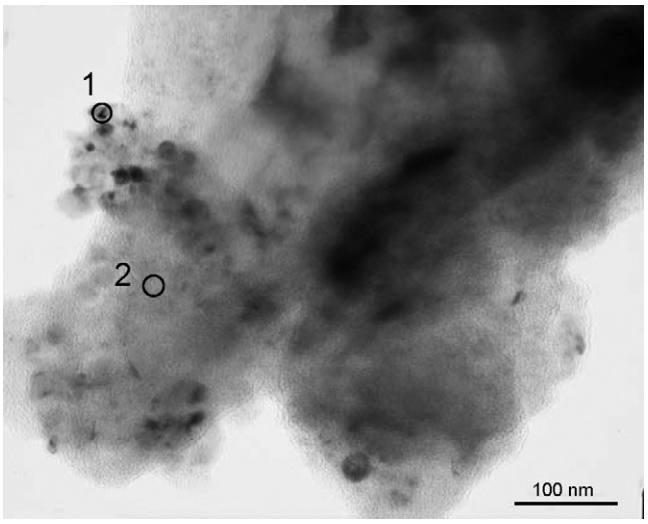

Fig. 2. TEM micrograph of the MgH_2–Ni^{nano} composite.

Next, we performed the TEM micrograph observation to see how the Ni elements were distributed on the surface of MgH_2 in a nanometer scale. Fig. 2 shows a TEM micrograph of the MgH_2–Ni^{nano} composite, where the particle size is estimated to be ~500 nm in diameter. Many black particles with smaller sizes than 20 nm are observed on the large bright particle. Table 1 shows the existing ratios of Mg and Ni elements evaluated from the EDX measurements, which are analyzed in spots with a diameter of 20 nm. Practically, O, C and Cu elements were also detected by the EDX analysis as well, where the C and Cu elements are originated from the sample holder. The trace of O element may be from a surface oxidation of MgH_2, which was already contaminated in the purchased sample. In the point 1 of Fig. 2 containing a black particle, the amount of Mg is as small as 12.5%, whereas the amount of Ni is as high as 87.5%. On the contrary, in point 2 without containing black particles, the existing ratio of Mg is much higher than that of Ni. This result indicates that the large particle is MgH_2 and the black particle is Ni doped in MgH_2 as a catalyst. Therefore, the particle size of Ni^{nano} in MgH_2 is estimated to be ~20 nm, which is the same size as that of Ni nano-particles doped as a starting material. Finally, from the above observations, it is concluded that the Ni^{nano} particles are uniformly distributed on the surface of the MgH_2 particles without agglomeration, which leads to fast kinetics we have reported so far [12].

Table 1
EDX analysis of the MgH_2–Ni^{nano} composite (1 and 2) and the MgH_2–Nb_2O_5 composites for as milled (3–8) and after dehydrogenation (9–12)

	Mg (mol%)	Ni (1 and 2), Nb (3–12) (mol%)
1	12.5	87.5
2	94.8	5.2
3	98.1	1.9
4	97.5	2.6
5	97.7	2.3
6	98.0	2.0
7	97.8	2.2
8	97.7	2.3
9	97.2	2.8
10	97.4	2.6
11	97.3	2.7
12	97.5	2.5

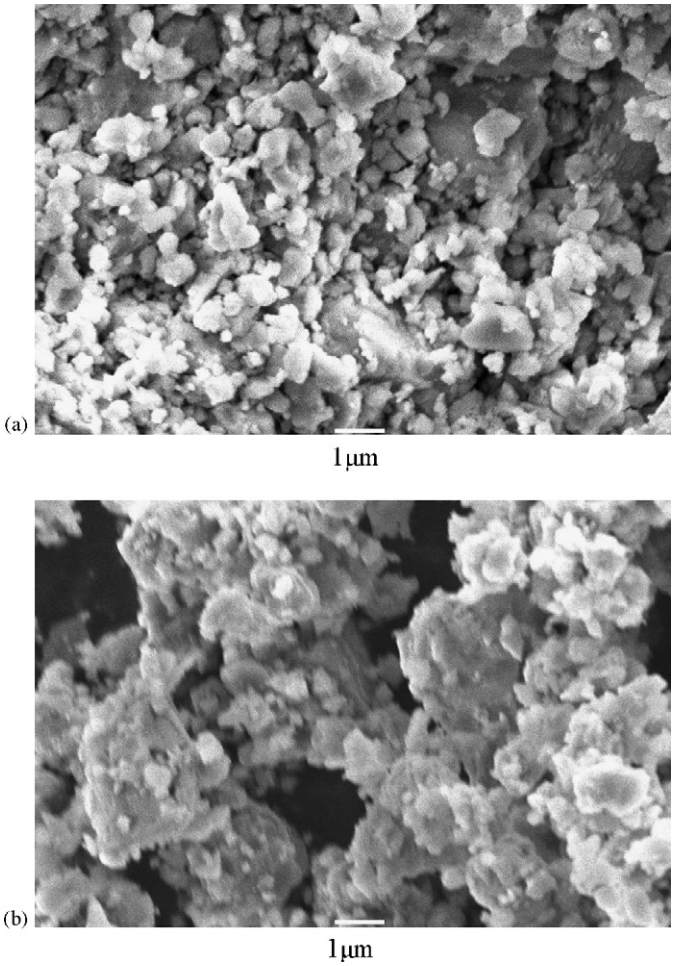

Fig. 3. Secondary electron (SE) micrographs of the MgH_2–Nb_2O_5 composite, in which (a) and (b) are, respectively, as milled and after dehydrogenation.

3.2. *Microstructure of MgH_2 catalyzed with Nb_2O_5 (MgH_2–Nb_2O_5 composite)*

Fig. 3(a) and (b) show the SE images of the MgH_2–Nb_2O_5 composite after ball-milling for 20 h at 400 rpm and after dehydrogenation, respectively. As shown in Fig. 3(a), particles with less than 1 μm in diameter mainly exist. The particle size is smaller than that of the MgH_2–Ni^{nano} composite, because the milling time is much longer in this case. After dehydrogenation as shown in Fig. 3(b), the SE image reveals that particles with a few micrometer size are formed by agglomeration of smaller particles than 1 μm by heating at 200 °C. In both the BSE images corresponding to Fig. 3(a) and (b) (not shown here), the contrast between the elements were not recognized. Therefore, it is concluded that the particles containing Nb elements cannot be distinguished within a micrometer scale by the SEM measurements.

It is important to perform the TEM observation to see how the additive Nb_2O_5 is distributed in the host MgH_2 particle in

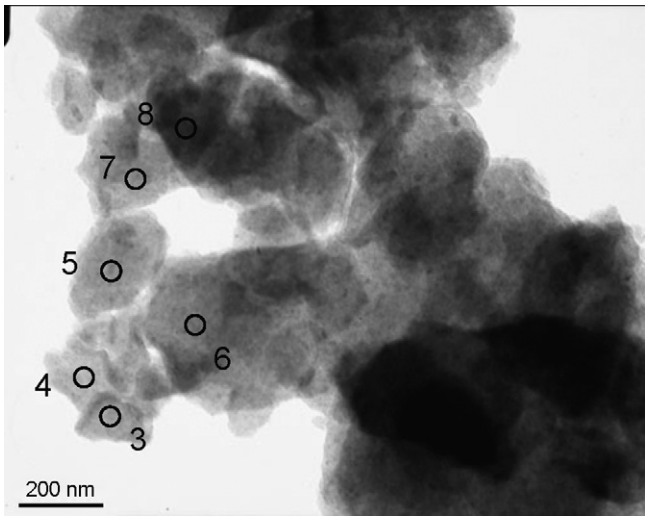

Fig. 4. TEM micrographs of the MgH_2–Nb_2O_5 composite.

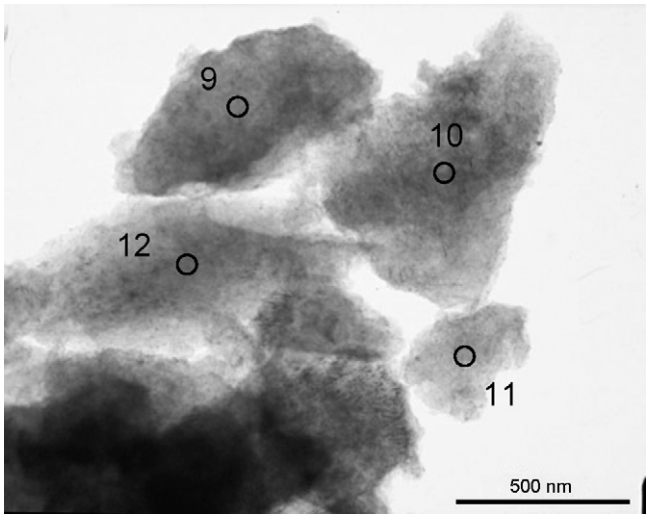

Fig. 6. TEM micrograph of the MgH_2–Nb_2O_5 composite after dehydrogenation.

a nanometer scale. Fig. 4 shows the TEM micrographs for the as-milled sample. It can be seen as a homogeneous distribution of the main particles with diameter of ∼200 nm in the photograph. Even in a much larger magnification, the particles corresponding to the additive were not detected (not shown here). As is evident from Table 1, the existing ratio of Mg to Nb is almost constant to be 98:2 within a diameter of 20 nm for all the points we performed the EDX analysis. This result indicates that the additive is uniformly dispersed in/on the MgH_2 particle as the shape of less than 10 nm particle. Friedrichs et al. also reported similar TEM images for MgH_2 milled for 15 min with 10 mass% Nb_2O_5 nano-powder, which showed fast kinetics of hydrogen desorption. However, the Nb-related particles in the sample were difficult to be distinguished from the MgH_2 phase [17].

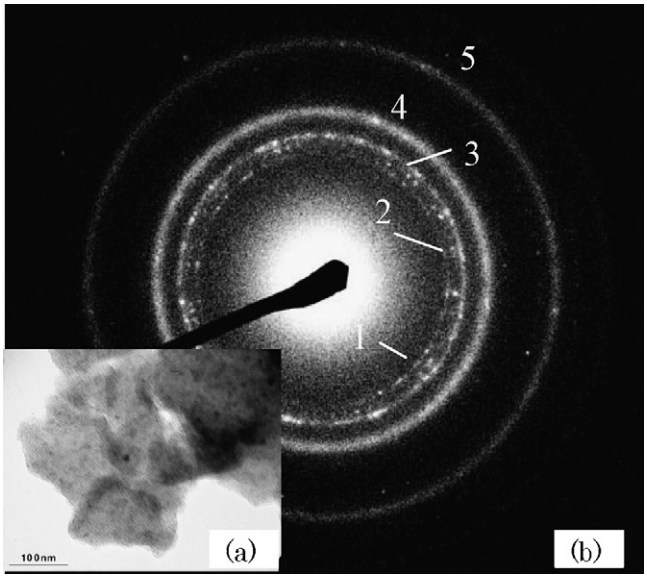

Fig. 5. TEM micrograph (a) and electron diffraction (ED) (b) of the MgH_2–Nb_2O_5 composite. Debye rings in ED are confirmed as follows, (1) Mg 100, (2) Mg 002, (3) Mg 101 and MgO 111, (4) MgO 200, (5) Mg 103 and MgO 220.

Fig. 5(a) and (b) show the TEM and electron diffraction (ED) micrographs in the same target area about the as-milled sample. In the ED micrograph (Fig. 5(b)), it is noted that there are only diffraction Debye rings. These rings correspond to the Mg and MgO phases. The XRD profile of the sample after ball-milling showed the MgH_2 and MgO phases as was observed in our previous work [13,14]. Therefore, the above results indicate that the hydrogenated sample released hydrogen gas during the TEM measurement under a high vacuum condition. The crystalline size of the Nb-related phase is too small to be detected as the diffraction rings.

Fig. 6 shows a TEM micrograph of the MgH_2–Nb_2O_5 composite after dehydrogenation. The particles with diameters of nearly 500 nm also homogeneously distribute in the micrograph. The EDX results as shown in Table 1 show that the existing ratios of Mg and Nb elements are almost the same for all the points we performed the EDX analysis. Therefore, the above result

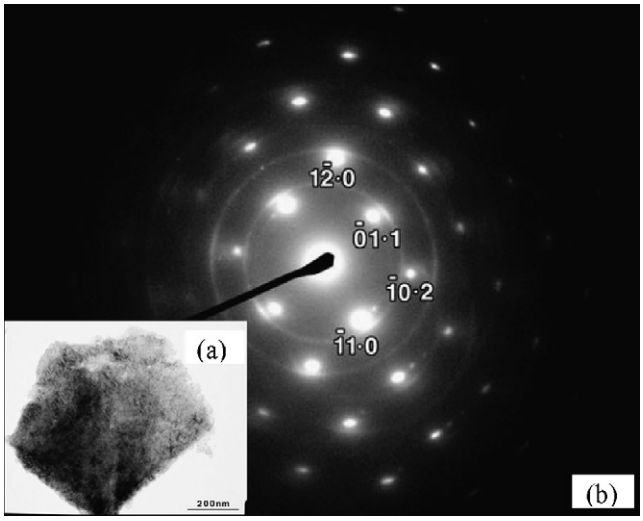

Fig. 7. TEM micrograph (a) and electron diffraction (ED) (b) of the MgH_2–Nb_2O_5 composite after dehydrogenation. Blemishs and Debye rings in ED are confirmed Mg and MgO, respectively.

indicates that the additive in the dehydrogenated Mg phase is still dispersed homogeneously in a nanometer scale even after heat treatment up to 200 °C, which leads to the fast kinetics for hydrogen absorption/desorption in Mg as we have reported [15]. Fig. 7(a) and (b) show the TEM and ED micrographs in the same target area about the sample after dehydrogenation. The diffraction spots and diffraction rings appear in ED micrograph of Fig. 7(b), which are confirmed to be the Mg and MgO phases, respectively. This result indicates that the crystalline size of Mg is grown into about 500 nm in diameter by heating up to 200 °C but the Nb particles do not grow to the size that can be identified by the present experimental conditions.

4. Conclusion

The microstructures of MgH_2 catalyzed with Ni nano-particle and Nb_2O_5 were investigated by SEM and TEM observations. Hydrogen desorption properties of both composites after the ball-milling have been examined and they showed almost the same properties, where the amount of ∼6.0 mass% hydrogen is desorbed in the temperature range from 150 to 250 °C at heating rate of 5 °C/min under He flow. However, the different distribution states of additives between two compounds are characterized as follows. For the MgH_2–Ni^{nano} composite, the metal Ni nano-particles are found in the BSE image. Ni particles with smaller diameters than 1 μm are uniformly distributed on the MgH_2 particles with smaller diameters than 5 μm. Furthermore, the TEM micrograph showed that the Ni particles are distributed to be ∼20 nm in diameter on MgH_2 uniformly, which is the same size as that of Ni^{nano} doped as a starting material. This may lead to the fast kinetics in this Ni-doped MgH_2 composite. On the other hand, for the MgH_2–Nb_2O_5 composite, the results of the TEM micrograph indicated that the particles corresponding to the additives are not detected anywhere. By EDX analysis in the spot with diameter of 20 nm, the ratio of Mg–Nb is evaluated to about 98:2, which is the same as the starting ratio. This result indicates that the additive particles are homogeneously distributed in/on the MgH_2 particle after ball-milling in a nanometer scale. Furthermore, regarding to the MgH_2–Nb_2O_5 composite, the product after dehydrogenation has absorbed gaseous hydrogen of ∼4.5 mass% even at room temperature under lower pressure than 1 MPa within 15 s. The additive particles in the composite after dehydrogenation were homogeneously distributed in the MgH_2 particles in a nanometer scale, while the crystalline size of Mg was grown into ∼500 nm in diameter. Such a uniform distribution of the additives may lead to the fast kinetics for hydrogen absorption in Mg.

Acknowledgement

This work was carried out by the Grant-in-Aid for COE Research (No. 13CE2002) of the Ministry of Education, Science and Culture of Japan.

References

[1] G. Liang, J. Huot, S. Boily, A. Van Neste, R. Schulz, J. Alloys Comp. 291 (1999) 295.
[2] G. Liang, J. Huot, S. Boily, A. Van Neste, R. Schulz, J. Alloys Comp. 292 (1999) 247.
[3] A. Zaluska, L. Zaluski, J.O. Ström-Olsen, J. Alloys Comp. 288 (1999) 217.
[4] J.-L. Bobet, B. Chevalier, M.Y. Song, B. Darriet, J. Etourneau, J. Alloys Comp. 336 (2002) 292.
[5] W. Oelerich, T. Klassen, R. Bormann, J. Alloys Comp. 315 (2001) 237.
[6] W. Oelerich, T. Klassen, R. Bormann, Adv. Eng. Mater. 3 (2001) 487.
[7] Z. Dehouche, T. Klassen, W. Oelerich, J. Goyette, T.K. Bose, R. Schulz, J. Alloys Comp. 347 (2002) 319.
[8] M.Y. Song, J.-L. Bobet, B. Darriet, J. Alloys Comp. 340 (2002) 256.
[9] J.-L. Bobet, S. Desmoulins-Krawiec, E. Grigorova, F. Cansell, B. Chevalier, J. Alloys Comp. 351 (2003) 217.
[10] G. Barkhordarian, T. Klassen, R. Bormann, Scripta Mater. 49 (2003) 213.
[11] G. Barkhordarian, T. Klassen, R. Bormann, J. Alloys Comp. 364 (2004) 242.
[12] N. Hanada, T. Ichikawa, H. Fuji, J. Phys. Chem. B 109 (2005) 7188.
[13] T. Ichikawa, N. Hanada, S. Isobe, H.Y. Leng, H. Fujii, Mater. Trans. 46 (2005) 1.
[14] N. Hanada, T. Ichikawa, H. Fujii, J. Alloys Comp. 404–406 (2005) 716.
[15] N. Hanada, T. Ichikawa, S. Hino, H. Fujii, J. Alloys Comp. 420 (2006) 46.
[16] N. Hanada, T. Ichikawa, T. Nakagawa, S. Isobe, H.Y. Leng, K. Tokoyoda, T. Honma, H. Fujii, J. Phys. Chem. B, in preparation.
[17] O. Friedrichs, J.C. Sánchez-López, C. López-Cartes, T. Klassen, R. Bormann, A. Fernández, J. Phys. Chem. B 110 (2006) 7845.